Since January 2020 Elsevier has created a COVID-19 resource centre with free information in English and Mandarin on the novel coronavirus COVID-19. The COVID-19 resource centre is hosted on Elsevier Connect, the company's public news and information website.

Bioorganic Chemistry 116 (2021) 105272

Contents lists available at ScienceDirect

Bioorganic Chemistry

journal homepage: www.elsevier.com/locate/bioorg

Synthesis of novel calcium channel blockers with ACE2 inhibition and dual antihypertensive/anti-inflammatory effects: A possible therapeutic tool for COVID-19

Shahenda Mahgoub [a,*], Mohamed-I Kotb El-Sayed [a,b], Mohamed F. El-Shehry [c], Samir Mohamed Awad [d], Yara E. Mansour [d], Samar S. Fatahala [d,*]

[a] Department of Biochemistry and Molecular Biology, Faculty of Pharmacy, Helwan University, P.O. Box, 11795 Cairo, Egypt
[b] Department of Biochemistry, Faculty of Pharmacy, Ahram Canadian University, Giza, Egypt
[c] Pesticide Chemistry Department, National Research Centre, P.O. Box, 12622 Dokki, Egypt
[d] Pharmaceutical Organic Chemistry Department, Helwan University, P.O. Box, 11795 Cairo, Egypt

ARTICLE INFO

Keywords:
Bioisosters
CCB
ACE2 receptor
COVID-19
THP-1 cells
Anti-inflammatory

ABSTRACT

Hypertension has been recognized as one of the most frequent comorbidities and risk factors for the seriousness and adverse consequences in COVID-19 patients. 3,4-dihydropyrimidin-2(*1H*) ones have attracted researchers to be synthesized *via* Beginilli reaction and evaluate their antihypertensive activities as bioisosteres of nifedipine a well-known calcium channel blocker. In this study, we report synthesis of some bioisosteres of pyrimidines as novel CCBs with potential ACE2 inhibitory effect as antihypertensive agents with protective effect against COVID-19 infection by suppression of ACE2 binding to SARS-CoV-2 Spike RBD. All compounds were evaluated for their antihypertensive and calcium channel blocking activities using nifedipine as a reference standard. Furthermore, they were screened for their ACE2 inhibition potential in addition to their anti-inflammatory effects on LPS-stimulated THP-1 cells. Most of the tested compounds exhibited significant antihypertensive activity, where compounds **7a, 8a** and **9a** exhibited the highest activity compared to nifedipine. Moreover, compounds **4a,b, 5a,b, 7a,b, 8a,c** and **9a** showed promising ACE2:SARS-CoV-2 Spike RBD inhibitory effect. Finally, compounds **5a, 7b** and **9a** exerted a promising anti-inflammatory effect by inhibition of CRP and IL-6 production. Ultimately, compound **9a** may be a promising antihypertensive candidate with anti-inflammatory and potential efficacy against COVID-19 *via* ACE2 receptor inhibition.

1. Introduction

Hypertension; a long-term medical condition in which the blood pressure in the arteries is persistently elevated, has been recognized as one of the most frequent comorbidities and risk factors for the seriousness and adverse consequences in COVID-19 patients [1]. Several drug classes have been used for the treatment of high blood pressure such as angiotensin converting enzyme (ACE)-inhibitors, diuretics, β-blockers, calcium channel blockers (CCBs) and others [2]. However, hyponatremia caused by diuretic therapy is considered a negative prognostic factor in COVID-19 patients [3]. On the other hand, ACE-inhibitors, β-blockers, angiotensin II (Ang II) receptor blockers and CCBs, depend on the synthesis of vasodilating prostaglandins to produce their effects [2]. CCBs were originally developed as potent vasodilators because of their ability to bind to and block calcium channels. This reduced calcium influx into the smooth muscle cells results in smooth muscle relaxation and vasodilation. They also alter heart rate to prevent peripheral and cerebral vasospasm and reduce chest pain caused by angina pectoris. Several studies have been performed to analyze the potential use of CCBs for treatment of a broad range of diseases from angina pectoris to different forms of dementia [4]. Nifedipine is one of the most common and classic calcium channel blockers. It is a first generation dihydropyridine and often used to reduce systemic vascular resistance and arterial pressure [4]. However, concerns on nifedipine focusing on its short half-life [5] and the rapid unpredictable fall in blood pressure. Consequently, precipitation in ischemic events, which led to the development of other CCB generations. In clinical practice, ACE inhibitors or Ang II type 1 receptor blockers are often used in combination with CCBs

* Corresponding authors.
E-mail addresses: Shahenda.Mahgoub@pharm.helwan.edu.eg (S. Mahgoub), Samar_Saleh@pharm.helwan.edu.eg (S.S. Fatahala).

https://doi.org/10.1016/j.bioorg.2021.105272
Received 31 May 2021; Received in revised form 11 August 2021; Accepted 14 August 2021
Available online 24 August 2021

to reach a sufficient antihypertensive effect [6], to prevent developing cardiovascular diseases or renal failure as blood pressure increases [7]. ACE inhibitors have been considered the first line treatment of hypertension, through inhibiting the hydrolysis of Ang I to the biologically active Ang II, as central regulators of the renin-angiotensin system (RAS). Ang II is the main vasoactive peptide in the RAS, acting as a strong vasoconstrictor, pro-inflammatory, pro-fibrotic, and anti-diuretic agent through its receptor AT1R. Subsequently, inhibition of the production of Ang II and its receptor-induced signaling, via AT1R blockers, have been highly effective therapies in hypertension [8].

On the other hand, ACE2 also is crucial in the modulation of blood pressure having an opposite effect to ACE [9]. ACE increases blood pressure by increasing the level of Ang II, while ACE2 decreases blood pressure and plays a critical physiologic role in the homeostasis of tissue microcirculation and inflammation [8,10,11]. ACE2 catalyzes the conversion of Ang II to Ang 1–7 and has direct effects on cardiac function along with several organs via counter-regulation of the RAS by lowering Ang II [10]. ACE2 is expressed on the plasma membranes of numerous cell types, like the alveolar and intestinal epithelia, cardiac and renal vascular endothelial cells, and on macrophages [8,11,12].

Unfortunately, membrane-bound ACE2 may also be targeted by virus like in severe COVID-19 cases, as it may act as a binding site for the virus spike proteins of SARS-CoV-1 and SARS-CoV-2 [13–16]. SARS-CoV-2 invasion unbalances the RAS, since viral cellular invasion and replication via ACE2, especially under conditions of enhanced ACE2 expression like hypertension, can lead to reduction of cell membrane-bound ACE2 through degradation of membranal ACE2 and increasing circulating ACE2. Thus, resulting in unbalanced paracrine action of Ang compounds, along with a local depletion of Ang 1–7, leaving Ang II activity unopposed, which leads to altered regional microcirculation, hypoxia, reactive oxygen species generation, endothelial damage, severe inflammation, hypercoagulability, tissue damage, and fibrosis [12]. Furthermore, unopposed Ang II activates NF-κB and proinflammatory cytokines release [17,18], along with activation of TNF-α/IL-6/ STAT-3 pathways [19]. Thus, inhibitors of ACE2 binding to SARS-CoV-2 Spike RBD may offer some protection against the viral infection and the inflammatory organ damage sequela [20].

Therefore, in this study, we hypothesized that CCBs with ACE2 inhibitory effect might exert an antihypertensive activity with protective effect against COVID-19 infection by suppression of ACE2 binding to SARS-CoV-2 Spike RBD.

The dihydropyridines (DHPs), and their prototype nifedipine, are still the most potent group of CCBs, used for the treatment of arterial hypertension. Nifedipine has been modified to improve its potency, safety, and duration of activity. Among structure modifications of DHPs, the bioisosters aza-analogs of DHPs, which gave rise to the

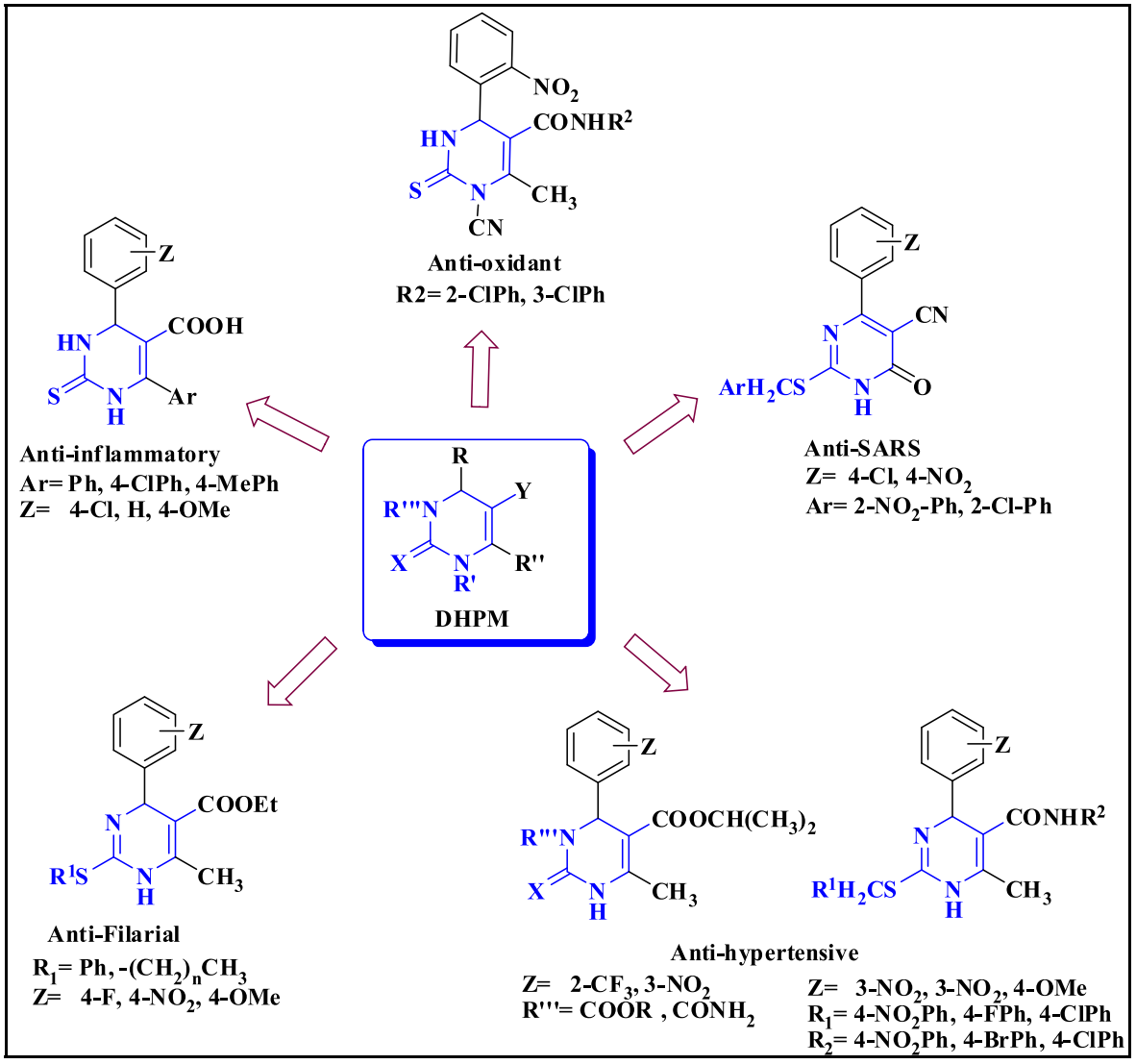

Fig.1. Dihydropyrimidines (DHPMs) as potent biologically active agents.

dihydropyrimidines (DHPMs) [21]. DHPMs are privileged heterocyclic scaffolds due to their biological and pharmaceutical activities as anti-inflammatory, anti-oxidant, anti-hypertensive, anti-filarial and anti-SARS [22–24], Fig. 1.

Moreover, recently some pyrimidinethiol compounds and their thioglycoside derivatives showed moderate *in vitro* anti-SARS-CoV-2 [25] and anti-avian influenza H5N1 virus [26] activities.

Motivated by the aforementioned discoveries, some bioisosteres of DHPMs were prepared and screened for their antihypertensive potential and ACE2 inhibition. Furthermore, their anti-inflammatory effects on LPS-stimulated THP-1 cells were evaluated. Here, we developed a program for the synthesis and evaluation of such nifedipine dihydropyridine bioisosteres, namely dihydropyrimidines (DHPMs) [22,23], as revealed in Fig. 2.

2. Results and discussion

2.1. Chemistry

As depicted in Scheme 1, the target compounds (**4**–**9**) were developed using a short and cost-effective route. Key considerations in the development of Dihydropyrimidine (DHPM) analogues were the ability to easily introduce structural variation at the C5 substituent. The target compounds were designed in such a way as to create diversity around the core skeleton using the easiest possible synthetic steps. Therefore, aldehydes and amines were chosen based upon their chemical character (i.e., electron-withdrawing and -polar groups).

Biginelli condensation protocol [27–30] is a one pot, three components coupling reaction of commercially available starting material thiourea, ethyl acetoacetate and selected aromatic aldehydes namely, *o*-cyano, *o*-chloro and *o*-bromobenzaldehyde in acid medium to afford the corresponding 1,4-dihydropyrimidine esters **4a-c**. Hence, saponification of the ethyl ester furnished the sodium salt of the 1,4-dihydropyrimidine analogues followed by acidification of the salts to pH ≈ 4, which provided the acids **5a-c**. The produced carboxylic acid derivatives were chlorinated with thionyl chloride to acyl chlorides **6a-c**. These acyl chlorides served as a template for the next reaction, in which the acylated derivatives were coupled with three aromatic amines namely, aniline, *p*-toluidine and *p*-fluoroaniline to produce the target 1,4-dihydropyrimidinethione carboxamide derivatives [31] **7a-c, 8a-c,** and **9a-c**. The purity of all the target compounds was confirmed using thin-layer chromatography (TLC) in different solvent systems and melting point techniques. The proposed structures were further confirmed by both the analytical and spectral data.

2.2. Biological evaluation

2.2.1. Evaluation of the antihypertensive activity

Pyrimidines and DHPMs, the important lead compounds for treatment of hypertension [32], have been developed as for **SQ 32926, SQ 32,547** and some pyrimidines analogues (Fig. 2 & Fig. 3). These compounds were proven to be orally active, with more potency and longer duration over the DHP antihypertensive drugs [33]. In the present study, nifedipine and the test compounds have similar bioisosteric nucleus, as revealed in (Fig. 2). Thus, all test compounds (**4**–**9**) were screened for their potential antihypertensive and calcium channel blocking (CCB) activities, using nifedipine as standard reference drug.

As presented in Table 1, all synthesized compounds; except compound **6c**; caused significant reduction in the mean arterial blood pressure (BP) compared to the control group. Compounds **7a** and **8a** displayed the most potent antihypertensive activity; almost equal to that of the standard nifedipine; with % reduction in BP reaching up to 29%, followed by **9a** (27%). While compounds **4a, 4b, 7b, 7c, 8b,** and **8c** showed moderated antihypertensive activity with % reduction in BP ranging from 22 to 23% along with compounds **4c** and **9c**, which demonstrated % decrease in BP about 21%. On the other hand, the rest of the compounds had lower antihypertensive potency.

SAR studies revealed that the 5-ethoxycarbonyl-2-thiopyrimidines derivatives **(4a-c)** showed comparable activity relative to nifedipine, while their hydrolysis decreased the activity as exemplified by carboxylic acid derivatives (**5a-c**). Meanwhile, when the later compounds were chlorinated by thionyl chloride, they gave acyl chlorides (**6a-c)** of weak antihypertensive activity. Conversely, amide derivatives (**7a-c, 8a-c,** and **9a-c**) retained the activity especially when bearing a **free phenyl moiety** as in compounds **7a**, **8a** and **9a,** which had promising activity compared to nifedipine, over the amidic group bearing **p-tolyl** substitution as in compounds **7b, 8b** and **9b**; or **4-florophenyl** substitution as in compounds **7c, 8c** and **9c**.

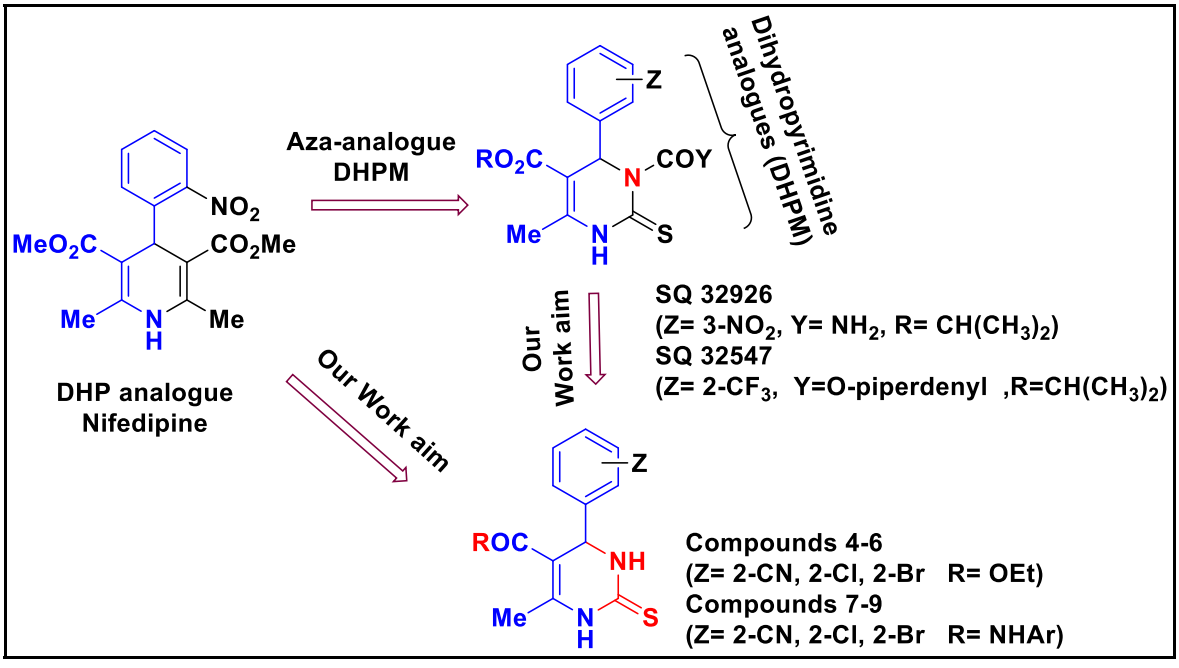

Fig. 2. DHP and its aza analogues bioisosteries. DHP: Dihydropyridine, DHPM: Dihydropyrimidine.

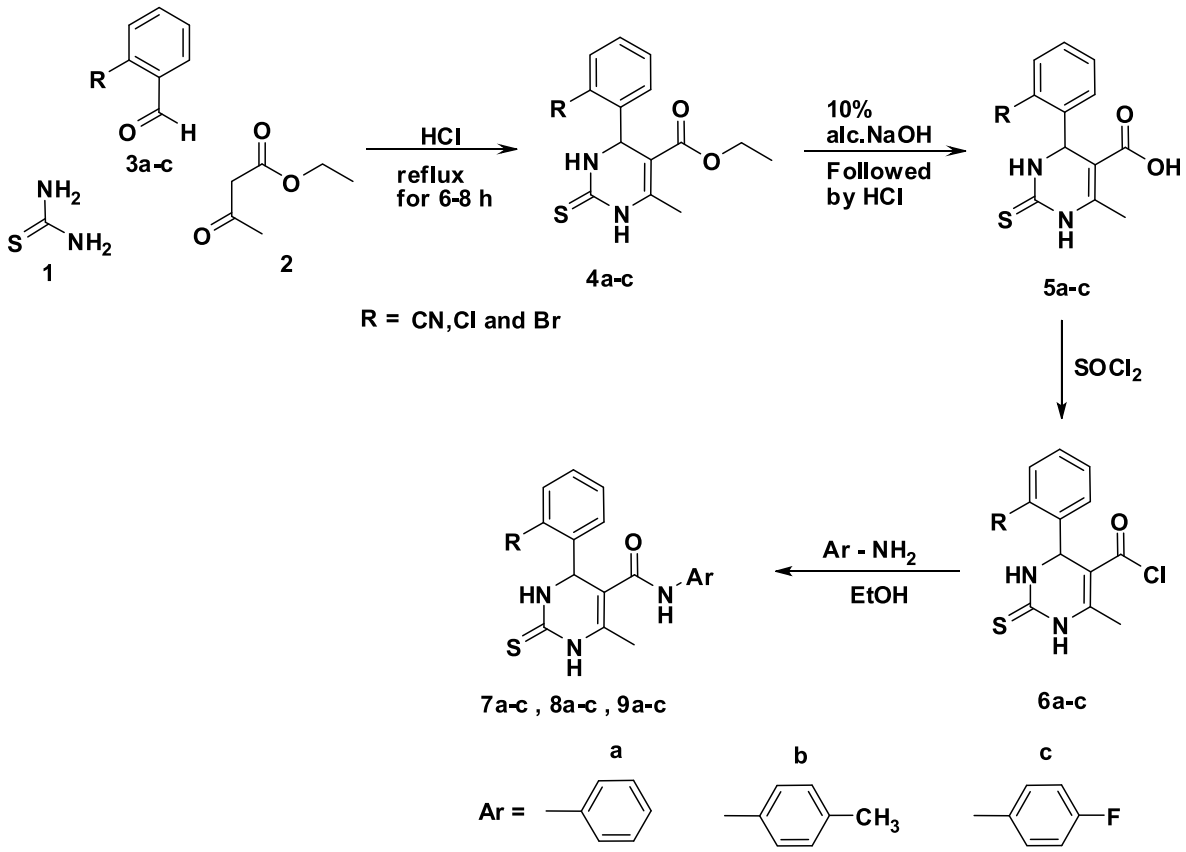

R \ Ar		CH3	F
CN	7a	7b	7c
Cl	8a	8b	8c
Br	9a	9b	9c

Scheme 1. Synthesis of dihydropyrimidines (DHPMs) **(4–9)**.

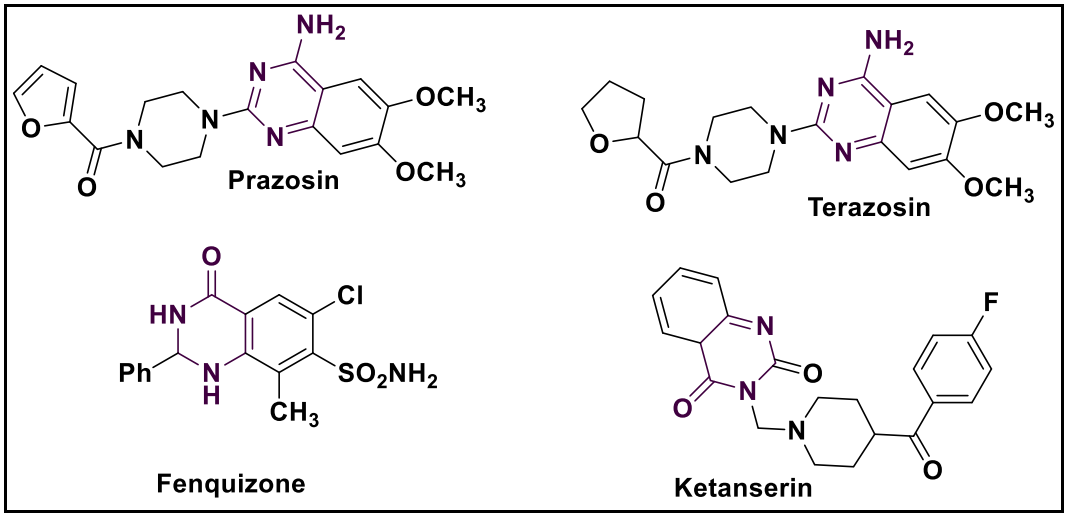

Fig. 3. Some potent antihypertensive agents containing pyrimidine moiety.

2.2.2. Calcium antagonism blocking activity in the isolated rat ileum.

In order to investigate the CCB blocking effect, the first approach was to study the effect of different synthetic derivatives on K^+ induced contracting isolated rat ileum. K^+ activates voltage-dependent Ca^{2+} channels to trigger this ion influx [34]. These changes in intracellular Ca^{2+} concentration regulate the contractility of the gastrointestinal

Table 1
Screening of Antihypertensive Activity.

Compound	Mean arterial BP (mm Hg)
Control	29.46 ± 0.54
4a	22.51 ± 1.11***
4b	22.68 ± 0.94***
4c	23.04 ± 0.97***
5a	24.70 ± 1.25***###
5b	24.81 ± 0.94***###
5c	23.82 ± 0.89***##
6a	26.98 ± 1.44*###
6b	25.37 ± 1.34***###
6c	27.58 ± 0.74###
7a	20.71 ± 0.68***
7b	22.84 ± 0.95***
7c	22.44 ± 0.96***
8a	20.92 ± 0.64***
8b	22.81 ± 1.13***
8c	22.86 ± 0.92***
9a	21.34 ± 1.34***
9b	23.47 ± 0.73***##
9c	23.07 ± 0.87***
Nifedipine	20.82 ± 0.58***

Data are expressed as mean ± SD. *, ***Significant from control group at $p < 0.05$ and 0.001, respectively. ##, ### Significant from Nifedipine group at $p <$ 0.01 and 0.001, respectively. BP: Blood pressure.

smooth muscles. All test compounds produced a decrease in the tone of ileal contractions in a dose dependent manner (0.5–0.1 mL), **(**Table 2**)**. As the relaxation of K^+ induced contractions by the tested compounds was similar to that caused by the standard drug nifedipine, thus the observed spasmolytic effect might be mediated through Ca^{2+} channel inhibition. The most active compounds were **7a**, **8a** and **9a** (IC_{50}, 19.65 ± 1.60, 20.23 ± 1.79, 21.45 ± 2.55 μg/mL, respectively), which was consistent with the potent antihypertensive activity produced by those compounds.

2.2.3. In vitro screening of ACE2: spike RBD (SARS-CoV-2) inhibitory effect

Overwhelmed by the serious outcomes of the coronavirus disease 2019 (COVID-19) pandemic, finding a potential tool to inhibit viral invasion and virulence is of greatest value. Antiviral treatment for COVID-19 is still a big challenge and investigations have not yet been able to find an adequately potent antiviral drug for SARS-CoV-2 infection. So far, many molecules have been explored to discover an efficient treatment [35]. ACE2 receptor; a part of the dual renin-angiotensin system (RAS) [36]; was found to be a key component in COVID-19 infection, and it is expressed on cell membranes of pulmonary and intestinal host cells. ACE2 serves as a receptor for initial viral homing, binding to COVID-19 spike-protein domains enabling viral entry into cells and subsequent replication [20]. ACE2 produces Ang 1–7, which plays a crucial role in counterbalancing the vasoconstrictive, pro-inflammatory, and pro-coagulant consequences of ACE-induced Ang II. Consequently, Ang 1–7 may drop in the tissues infected by COVID-19, leading to unrestrained deleterious effects of Ang II [37].

Thus, in this study all the synthesized compounds were screened for their inhibitory effect on ACE2 aiming to find antihypertensive compounds with inhibitory ACE2 potency thus, block the binding anchor for COVID-19 spike-protein domains. The results showed that out of 18 derivatives, nine showed promising inhibitory activity against ACE2, **(**Table 3**)**. The most active ACE2 inhibitory compounds were **4a** and **5a** (IC_{50}, 8.5 ± 0.92 and 9.8 ± 1.06 nM, respectively). Compounds **8a, 7b,** and **7a** showed strong inhibitory effects (IC_{50}, 10.6 ± 0.61, 10.8 ± 0.75 and 11.6 ± 0.94 nM, respectively), followed by **4b**, **5b**, **8c** (IC_{50}, ~12.5 nM) and **9a** (IC_{50}, 13.7 ± 1.37 nM). Hence, we can recognize the effect of the electron withdrawing group 4-(2-Cyanophenyl) in C4, as in compounds **4a** (ester), **5a** (acid) and **7a** (amide), which exhibited the highest ACE2 inhibitory activity, over 2-halophenyl as in compounds **4c**, **5c**, **7c**, **8c** and **9b,c**, which showed moderate to no activity. Thus, the activity among compounds **4a, 5a, 7a** and **7b** could be attributed to the more polar cyano group over the electron withdrawing effects of the less polar halo groups (chloro and bromo) in compounds **7c, 8b,c** and **9b,c**.

Regarding the anti-SARS-CoV-2 activity of the synthesized DHPMs analogues shown in our study, *Abu-Zaied et al.* revealed that some pyrimidinethiol compounds and their thioglycoside derivatives showed moderate *in vitro* anti-SARS-CoV-2 activity [25]. Also, Abu-Zaied and coworkers, assessed some synthesized cytosine thioglycoside analogues for their *in vitro* activity against avian influenza H5N1 virus and those derivatives displayed high to moderate activity [26].

The THP-1 cell line has been widely used to study immune responses [38] as an *in vitro* model of macrophages in studies of macrophage involvement in inflammatory responses. It is differentiated by using Phorbol 12-myristate 13-acetate (PMA) and activated by bacterial

Table 2
Screening of Ca^{2+} channel blocking activity of different synthetic compounds and nifedipine on K^+ (80 mM)-induced contractions of rat ileum.

Compound	IC_{50} (μg/ml)
4a	23.07 ± 1.53
4b	24.69 ± 2.35
4c	23.62 ± 2.33
5a	24.37 ± 1.45
5b	25.25 ± 1.39
5c	24.81 ± 1.94
6a	26.84 ± 1.51
6b	30.78 ± 2.52
6c	29.73 ± 2.44
7a	19.65 ± 1.60
7b	22.81 ± 2.46
7c	22.85 ± 1.11
8a	20.23 ± 1.79
8b	22.91 ± 2.59
8c	22.63 ± 1.99
9a	21.45 ± 2.55
9b	22.43 ± 1.83
9c	22.57 ± 2.39
Nifedipine	21.00 ± 1.20

Data are expressed as mean ± SD for three independent experiments.

Table 3
Effect of synthetized derivatives on ACE2:SARS-CoV-2 Spike (RBD) inhibition.

Compound	IC_{50} (nM)
4a	8.50 ± 0.92
4b	12.50 ± 1.13
4c	23.00 ± 1.00
5a	9.80 ± 1.06
5b	12.50 ± 1.35
5c	18.40 ± 1.05
6a	17.50 ± 1.31
6b	23.70 ± 1.35
6c	16.50 ± 1.08
7a	11.60 ± 0.94
7b	10.80 ± 0.75
7c	20.10 ± 1.10
8a	10.60 ± 0.61
8b	19.20 ± 1.11
8c	12.50 ± 1.08
9a	13.70 ± 1.37
9b	15.50 ± 1.37
9c	21.60 ± 0.92

Data are presented as mean ± SD of three independent experiments.
ACE2: Angiotensin-converting enzyme 2, SARS-CoV-2: severe acute respiratory syndrome coronavirus, RBD: Receptor-binding domain.

lipopolysaccharides (LPS). Activated THP-1 cells secrete inflammatory cytokines as a result of cell signaling cascade events stimulated by LPS. Cytokines expression levels are considered valuable physiological readouts for cell-based models of inflammation [39] that could help to assess the activities of anti-inflammatory compounds. Since COVID-19 pandemic, many anti-viral drugs have been tested for COVID-19 management; however, none were proven to be fully effective. On the other hand, management of the complications caused mainly by inflammation has shown to be the potential key for better survival rates and shorter hospitalization period for COVID-19 patients. Therefore, several FDA approved drugs for different diseases were tested as current or potential therapies for the treatment or management of COVID-19 through their direct or indirect anti-inflammatory actions. In addition to the investigation of their ability to interact with ACE2 [40].

In the present study, we assessed some of the synthetized derivatives for their anti-inflammatory effects using THP-1 cells stimulated with LPS.

2.2.4. Cytotoxic effect of different compounds against PMA-differentiated THP-1 Cells.

The most active compounds with potential ACE2 inhibitory activity *viz* **4a,b, 5a,b, 7a,b, 8a,c** and **9a** were tested for their cytotoxic effect on PMA-differentiated THP-1 cells. Results are shown in (Table 4**)** and demonstrated that compound **7b** (amidic moiety bearing polar methyl group) was the most toxic with IC_{50} value of 61 μM. Compounds **5a** (bearing both cyano and acidic moities),**7a, 8a,** and **9a** (amidic moiety bearing hydrophobic phenyl group) showed less cytotoxic effect on THP-1 cells. While, compounds **5b** (bearing polar acidic moiety) and **4a** (ester group) gave the lowest toxicity at 342 and 533 μM, respectively. Compounds **5a**, **7a,b** and **9a** were the final selected compounds used for cytokine production assessments to study their activity as anti-inflammatory agents and were used below their corresponding IC_{50} values (1/4 IC_{50}).

2.2.5. Effect of the selected compounds on pro-inflammatory cytokine IL-6 and CRP production

Macrophages differentiate into various subpopulations with diverse functions in response to various microbial and environmental signals. These cell subpopulations are vital for the inflammatory process and the defence mechanism against infections via the secretion of inflammatory cytokines, such as TNF-α, and IL-6 [41].

However, over-secretion of these mediators has been noticed in several inflammatory diseases including the recent pandemic COVID 19 in which hyper-inflammatory response prompted by severe acute respiratory syndrome coronavirus 2 (SARS-CoV-2) is a foremost cause of disease severity and mortality [42,43]. On the other hand, elevated C-reactive protein (CRP), which is an acute-phase protein synthesized in the liver in response to IL-6 and a widely available biomarker of inflammation [44], is associated with cardiovascular disease [45], pneumonia [46], inflammatory rheumatic diseases as well as severe H1N1 influenza [47]. CRP was reported as a procoagulant with implications for atherothrombosis [48]. Recently, several studies have reported an association between higher CRP level and greater disease severity in COVID-19 patients [49,50]. Moreover, higher CRP concentrations were associated with mortality [51]. From the classic drugs that have been screened for their effect to control COVID-19, the old known antimalarial drugs, chloroquine, and hydroxy chloroquine. They showed to possess direct anti-inflammatory effect *via* inhibition of IL-1 and IL-6 production by monocytes [52]. Moreover, when applied to RBD–ACE-2 using molecular docking studies, they showed a potential ability to interfere with the initial attachment of virus particles to the respiratory tract epithelium [53]. Also, hydroxychloroquine in combination with azithromycin has been suggested for COVID-19 treatment through decreasing viral replication along with the anti-inflammatory effect [35]. Moreover, combination of umifenovir with lopinavir/ritonavir showed good antiviral activity against SARS-CoV-2 [43].

Regarding the use of CCBs in COVID-19 patients, a small retrospective study was performed on elderly hospitalized COVID-19 patients with hypertension treated or not treated with either nifedipine or amlodipine. Treatment with either CCBs was found to be significantly correlated with an improved mortality, and a reduced risk for mechanical ventilation in those patients. However, levels of CRP and IL-6 were not significantly different between the two groups. Therefore, the vasodilatory CCBs mentioned in the referred study may improve clinical outcomes in COVID-19 patients. Nevertheless, they should be accompanied with anti-inflammatory agents [54].

Hence, our biological evaluation journey of the synthesized compounds ended by assessing the selected compounds **5a, 7a,b,** and **9a** for their potential *in vitro* anti-inflammatory activity in LPS-stimulated THP-1 cells through measuring the levels of IL-6 and CRP.

Results revealed that the secretion of IL-6 by LPS-stimulated THP-1 cells in response to all selected test compounds was significantly lower than in the cells stimulated with LPS (positive control), **(**Fig. 4**)**.

Table 4
Effect of different derivatives against THP-1 cells viability.

Compound	IC_{50}, μg/ml (IC_{50} μM)
4a	1551.50 ± 134.30 (533)
4b	697.60 ± 65.60 (231)
4c	ND
5a	496.10 ± 38.70 (118)
5b	967.10 ± 79.20 (342)
5c	ND
6a	ND
6b	ND
6c	ND
7a	433.70 ± 32.90 (123)
7b	222.40 ± 10.10 (61)
7c	ND
8a	464.20 ± 29.70 (125)
8b	ND
8c	790.60 ± 58.60 (197)
9a	484.90 ± 3.24 (116)
9b	ND
9c	ND

Data are presented as mean ± SD of three independent experiments.
Value between ( ) is IC_{50} in μM. ND: Not determined.
THP-1: Human monocytic cell line.

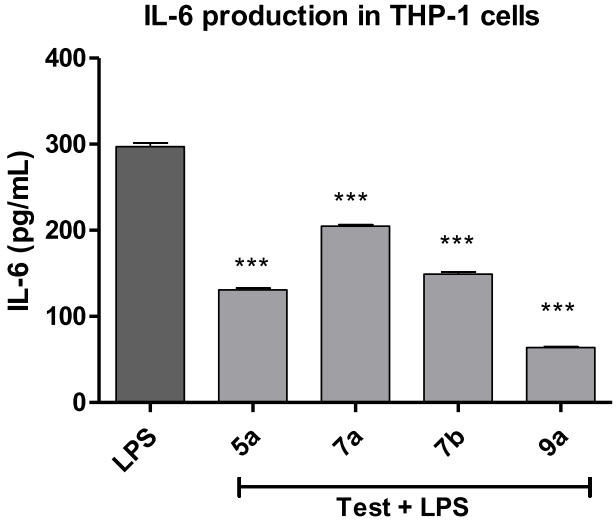

Fig. 4. Effect of the selected compounds on IL-6 production by PMA-differentiated THP-1 cells in the presence of LPS (0.5 μg/mL). ***: Significant ($p < 0.001$) compared to LPS. Data are presented as mean ± SD, ($n = 3$). IL-6: Interleukine-6, LPS: Lipopolysaccharide, THP-1: Human monocytic cell line.

Compounds **5a** and **9a** showed the greatest effect on the cytokine level with a reduction reaching about 56% and 79%, respectively, followed by **7b** (47%). However, compound **7a** had the lowest effect on the level of this cytokine.

Regarding the level of CRP in LPS-stimulated THP-1 cells in response to the treatment by compounds **5a, 7a,b** and **9a,** it was significantly lower when compared to its level in the cells stimulated with LPS (positive control), **(**Fig. 5**)**. The greatest effect on CRP level was exhibited by compound **9a,** which caused about 95% decrease in the level of CRP, while treatment with compounds **5a** and **7b** showed moderate decrease in CRP production. However, **7a** showed no significant effect on the level of this prototypic marker of inflammation.

Based on the cytokine production and anti-inflammatory performance, these remarkable results highlight the spectacle promising activity of compounds **5a** (free acidic group) and **9a** (amidic group bearing hydrophobic phenyl and aryl group in C4 bearing 2-Bromo group).

The biological activity exhibited by the test compounds, suggested that the amidic group is a key element for CCBs activity as for compounds **7a, 8a** and **9a**. In meanwhile, the ester in **4a** and acid in **5a** is a predominant factor for ACE2 inhibitory activity, where both bearing an electron withdrawing group (2-CN) in C4 aryl. Yet, amidic group in **7a, 8a** and **9a** showed strong inhibitory activity against ACE2, but less than acidic and ester. For anti-inflammatory activities, acid in **5a** and amidic in **7b, 8a** and **9a** showed the highest effect. The 4-flouro group in the amidic moieties of compounds **7c, 8c** and **9c** masked the activity of these tested compounds, as revealed in Fig. 6.

3. Conclusion

In this study, we have presented novel DHPMs analogues that can act as both CCBs and ACE2 inhibitory agents, for the treatment of elevated BP. In addition, some of these scaffolds showed potential anti-inflammatory activities *via* reduction of IL-6 and CRP production in LPS-stimulated THP-1 cells, with a much potent profile. The outcomes of this study may pave the way to find an effective therapeutic tool for hypertensive patients with a protective effect against COVID-19 infection coupled with anti-inflammatory activities.

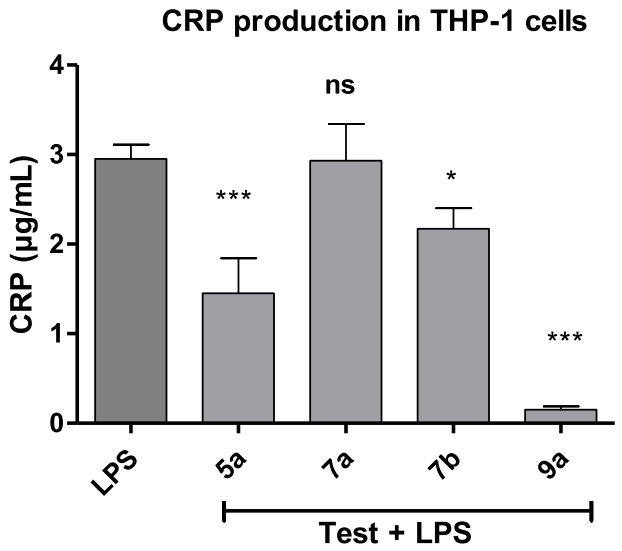

Fig. 5. Effect of the selected compounds on CRP production by PMA-differentiated THP-1 cells in the presence of LPS (0.5 µg/mL). *, ***: Significant at $p < 0.05$ and 0.001, respectively compared to LPS. Data are presented as mean ± SD, ($n = 3$). ns: not significant. CRP: C-Reactive Protein, LPS: Lipopolysaccharide, THP-1: Human monocytic cell line.

4. Experimental

4.1. Chemistry

4.1.1. Material and methods

All the reagents and solvents were purchased from Merck (Darmstadt, Germany) and used without further purification. All melting points were uncorrected and measured using Electro-thermal IA 9100 apparatus (Shimadzu, Japan). ^{1}HNMR spectra were recorded on Bruker AMX400 and Bruker Current AV400 Data spectrometer (400 MHz), Bruker BioSpin GmbH, Germany. Spectra and chemical shifts (δ) were expressed as ppm against TMS as internal reference. ESI mass spectra with a Finnigan Thermo Quest MAT 95XL spectrometer and FAB high-resolution (HR) mass spectra with a VG Analytical 70-250S spectrometer; Palmer, USA; using an MCA method and polyethylene glycol as a support. The reactions were monitored by thin layer chromatography (TLC) analysis using silica gel (60 F254) –coated aluminium plates (Merck) which were visualized by UV irradiation (254 nm) and iodine vapors. Column chromatography was performed by using silica gel (60–120 mesh). All reactions were carried out under dry nitrogen. Compounds **4b** [55–57], **4c** [58], **5b** [59], **8a** [60] **8c** [61] were previously prepared. Their melting points and characterization data are in agreement with the published references. Compounds **9a-c** are commercially available [62–64].

Ethyl-6-methyl-4-(2-substituted phenyl)-2-thioxo-1,2,3,4-tetrahydro pyrimidine-5-carboxylate 4a-c:

A mixture of thiourea 1 (7.6 g, 0.1 mol), ethyl acetoacetate 2 (13 mL, 0.1 mol) and the appropriate aromatic aldehyde 3 (0.1 mol) in 50 mL absolute ethanol containing 1 mL of 37% HCl was refluxed for 8 h. The reaction mixture was cooled then poured on to a mixture of ice/water and neutralized with ammonia solution. The produced precipitate was filtered off, dried under suction and re-crystallized from ethanol.

Ethyl-4-(2-cyanophenyl)-6-methyl-2-thioxo-1,2,3,4-tetrahydropyrimidine-5-carboxylate 4a:

Yield: 76%; m.p.: 252–254 °C; IR ν (KBr cm^{-1}): 3357 (NH), 3173 (CH, aromatic), 2978 (CH, aliphatic), 2224 (CN), 1683 (C═O), 1277 (C═S), 1220(C—O). ^{1}HNMR (DMSO-d_6, 400 MHz) δ: 1.5 (t, 3H, CH_3 CH_2-O), 2.5 (s, 3H, CH_3), 4.1 (q, 2H, CH_3CH_2-O), 5.6 (s, 1H, CH), 7.2–7.5 (m, 4H, aromatic), 8.4, 9.9 (2 s, 2H, 2NH (D_2O exchangeable)). ^{13}C NMR: (DMSO-d_6, 400 MHz) δ (ppm) 174.75, 167.75, 160.62, 145.52, 133.75, 132.29, 128.79, 127.66, 111.65, 105.79, 59.59, 54.4, 18.2, 14.5; MS (EI) *m/z*: 301.11 (M^+, 16.5%); Anal. Calcd., for $C_{15}H_{15}N_3O_2S$: C, 59.78; H, 5.02; N, 13.94. Found: C, 59.68; H, 5.17; N, 13.86.

Ethyl-4-(2-chlorophenyl)-6-methyl-2-thioxo-1,2,3,4-tetrahydropyrimidine-5-carboxylate 4b:

Yield: 69%; m.p.: 220–222 °C.

Ethyl-4-(2-bromophenyl)-6-methyl-2-thioxo-1,2,3,4-tetrahydropyrimidine-5-carboxylate 4c:

Yield: 70%; m.p.: 202–204 °C.

6-Methyl-4-(2-substituted phenyl)-2-thioxo-1,2,3,4-tetrahydropyrimidine-5-carboxylic acid 5a-c:

A solution of any of **4a-c** (3.6 g, 0.01 mol) in 50 mL of 10% alcoholic NaOH was refluxed for 2 h. Then was cooled and acidified with conc. HCl, the precipitate was filtered off, washed with water, dried under suction, and recrystallized from ethanol.

4-(2-cyanophenyl)-6-methyl-2- thioxo-1,2,3,4-tetrahydropyrimidine -5-carboxylic acid 5a:

Yield: 77%; m.p.: 241–243 °C; IR ν (KBr cm^{-1}): 3451 (OH), 3334 (NH), 3170 (CH, aromatic), 2979 (CH, aliphatic), 2226 (CN), 1690 (C═O), 1270 (C═S), 1225 (C—O). ^{1}HNMR (DMSO-d_6, 400 MHz)δ: 2.5 (s, 3H, CH_3), 5.3 (s, CH, pyrimidine), 7.3–7.5 (m, 4H, aromatic), 7.6, 10.00 (2 s, 2H, 2NH (D_2O exchangeable)), 12.00 (s, 1H, COOH (D_2O exchangeable)). ^{13}C NMR: (DMSO-d_6, 400 MHz) δ (ppm) 178.12, 169.70, 154.70, 147.57, 139.03, 129.30, 128.40, 126.03, 125.49, 116.84, 114.96, 79.70, 15.09; MS (EI) *m/z*: 273.13 (M^+, 14.7%), Anal. Calcd., for $C_{13}H_{11}N_3O_2S$: C, 57.13; H, 4.06; N, 15.37. Found: C, 57.09; H,

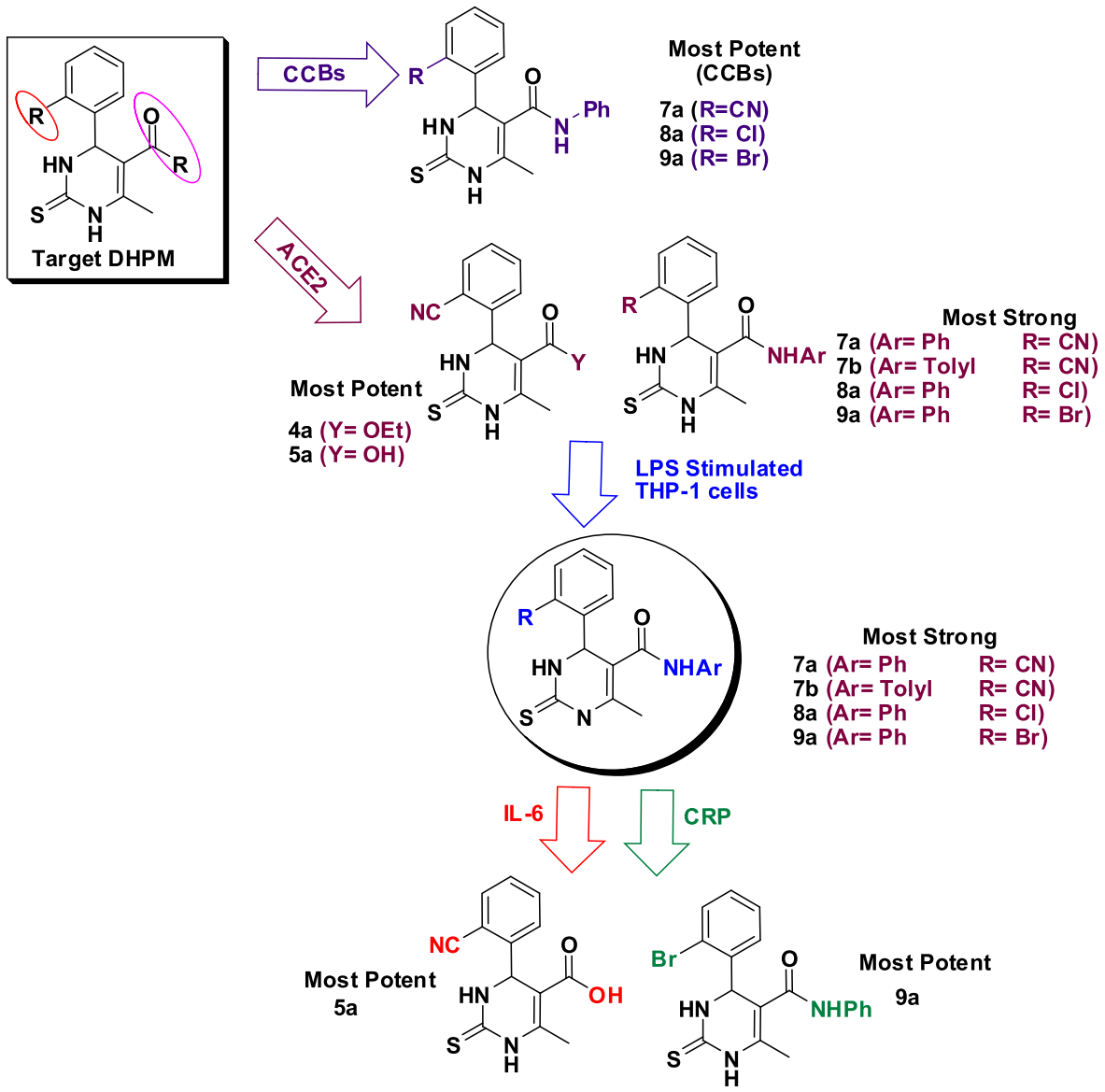

Fig. 6. SAR for the most potent compounds. DHPMs: Dihydropyrimidines, CCBs: calcium channel blockers, ACE2: Angiotensin-converting enzyme 2, THP-1: Human monocytic cell line, IL-6: Interleukine-6, LPS: Lipopolysaccharide, CRP: C-Reactive Protein.

4.17; N, 15.45.

4-(2-chlorophenyl)-6-Methyl-2-thioxo-1,2,3,4-tetrahydropyrimidine-5-carboxylic acid 5b:

Yield: 67%; m.p.: 210–212 °C.

4-(2-bromophenyl)-6-methyl-2-thioxo-1,2,3,3-tetrahydropyrimidine-5-carboxylic acid 5c:

Yield: 65%; m.p.: 239–241 °C; IR ν (KBr cm^{-1}): 3372 (OH), 3247 (NH), 3173 (CH, aromatic), 2973 (CH, aliphatic), 1687 (C═O), 1271 (C═S), 1229 (C—O). ^{1}HNMR (DMSO-d_6, 400 MHz) δ: 2.5 (3H, CH_3, pyrimidine), 5.1 (s, 1H, CH, pyrimidine), 7.3–7.4 (m, 4H, aromatic), 9.7, 10.2 (2 s, 2H, 2NH (D_2O exchangeable)), 11.5 (s, 1H, COOH (D_2O exchangeable)), ^{13}C NMR: (DMSO-d_6, 400 MHz) δ (ppm) 179.34, 168.76, 160.43, 145,32, 131.75, 129.30, 128.40, 121.49, 106.45, 56.05, 19.05; MS (EI) m/z: 325.82 (M^+, 34.9%), 327.91 (M + 2, 33.1%) Anal. Calcd., for $C_{12}H_{11}BrN_2O_2S$: C, 44.05; H, 3.39; N, 8.56. Found: C, 44.12; H, 3.53; N, 8.67.

6-Methyl-4-(2-substituted phenyl)-2-thioxo-1,2,3,4-tetrahydropyrimidine-5-carbonyl chloride 6a-c:

A mixture of any of **5a-c** (3.6 g, 0.01 mol) and 15 mL thionyl chloride was refluxed for 40 min. Unreacted thionyl chloride was removed by heating the reaction mixture on water bath. The produced acid chlorides **6a-c** were rapidly dried under suction and used as a crude for subsequent work.

6-Methyl-4-(2-cyanophenyl)-2-thioxo-1,2,3,4-tetrahydropyrimidine-5-carbonyl chloride 6a:

Yield: 61%; m.p.: 276–278 °C: IR ν (KBr cm^{-1}): 3340 (NH), 3185 (CH, aromatic), 2983 (CH, aliphatic), 2250 (CN), 1775 (C═O), 1270 (C═S), ^{1}HNMR (DMSO-d_6, 400 MHz) δ: 2.5 (s, 3H, CH_3), 5.2 (s, 1H, CH, pyrimidine), 7.2–7.4 (m, 4H, aromatic), 9.6,10.0 (s, 2NH, D_2O exchangeable). MS (EI) m/z: 291.75 (M^+, 16.0%), (M + 2, 5.3%), Anal. Calcd., for $C_{13}H_{10}ClN_3OS$: C, 53.52; H, 3.45; N, 14.40. Found: C, 53.19; H, 3.47; N, 14.37.

6-Methyl-4-(2-chlorophenyl)-2-thioxo-1,2,3,4-tetrahydropyrimidine-5-carbonyl chloride 6b:

Yield: 71%; m.p.: 263–265 °C; IR ν (KBr cm^{-1}): 3297 (NH), 3181 (CH, aromatic), 2985 (CH, aliphatic), 1772 (C═O), 1270 (C═S). ^{1}HNMR (DMSO-d_6, 400 MHz) δ: 2.4 (s, 3H, CH_3), 2.4 (s, 3H, CH_3), 5.2 (s, 1H, CH, pyrimidine), 7.5–7.8 (m, 4H, aromatic), 8.9, 9.3 (s, 2NH, D_2O exchangeable). MS (EI) m/z: 301.19 (M^+, 22.8%), (M + 2, 7.6%) Anal. Calcd., for $C_{12}H_{10}Cl_2N_2OS$: C,47.85; H, 3.35; N, 9.30. Found: C, 47.67;

H, 3.47; N, 9.40.

6-Methyl-4-(2-bromophenyl)-2-thioxo-1,2,3,4-tetrahydropyrimidine-5-carbonyl chloride 6c:

Yield: 67%; m.p.: 250–252 °C; IR ν (KBr cm^{-1}): 3258 (NH), 3187 (CH, aromatic), 2982(CH, aliphatic), 1787 (C═O), 1271(C═S). ^{1}HNMR (DMSO-d_6, 400 MHz) δ: 2.4 (3H, CH_3, pyrimidine), 5.6 (s, 1H, CH, pyrimidine), 7.1–7.6 (m, 4H, aromatic), 9.5, 9.7 (s, 2NH, D_2O exchangeable). MS (EI) *m/z*: 345.64 (M^+, 11.3%), (M + 2, 3.7%). Anal. Calcd., for $C_{12}H_{10}BrClN_2OS$: C, 41.70; H, 2.92; N, 8.10. Found: C, 41.58; H, 2.83; N, 8.20.

6-Methyl-4-(2-substituted phenyl)-*N*-substitutedphenyl-2-thioxo-1,2,3,4-tetrahydropyrimidine-5-carboxamide 7a-c, 8a-c, and 9a-c:

A mixture of any **6a-c** (0.76 g, 0.01 mol) and the appropriate aromatic amine (0.01 mol) in 25 mL ethanol was refluxed for 5hrs, then cooled, filtered off, dried, and recrystallized from ethanol.

4-(2-cyanophenyl)-6-methyl-*N*-phenyl-2-thioxo-1,2,3,4-tetrahydropyrimidine-5-carboxamide 7a:

Yield: 77%; m.p.: 263–264 °C; IR ν (KBr cm^{-1}): 3343, 3230 (NH), 3178 (CH, aromatic), 2973 (CH, aliphatic), 1671 (C═O), 1270 (C═S). ^{1}HNMR (DMSO-d_6, 400 MHz) δ: 2.4 (s, 3H, CH_3), 5.7 (s, 1H, CH-pyrimidine), 7.5–8.1 (m, 9H, aromatic), 8.0, 9.3 (2 s, 2H, 2NH (D_2O exchangeable)), 9.2 (s, 1H, CONH (D_2O exchangeable)). ^{13}C NMR: (DMSO-d_6, 400 MHz) δ (ppm): 174.12, 163.23,159.45, 145.57, 137.72, 132.84, 132.66, 128,45, 127.6, 127.43, 121.61, 115.64, 111.92, 106.42, 53.43, 19.53; Calcd., for $C_{19}H_{16}N_4OS$: C, 65.50; H, 4.63; N, 16.08. Found: C, 65.62; H, 4.52; N, 16.12.

4-(2-cyanophenyl)-6-methyl-*N*-(4-methylphenyl)-2-thioxo-1,2,3,4-tetrahydropyrimidine-5-carboxamide 7b:

Yield: 70%; m.p.: 276–278 °C; IR ν (KBr cm^{-1}): 3357, 3260 (NH), 3152 (CH, aromatic,), 2987 (CH, aliphatic), 1673 (C═O), 1270 (C═S). ^{1}HNMR (DMSO-d_6, 400 MHz) δ: 2.3 (s, 3H, CH_3), 2.9 (s, 3H, CH_3), 5.2 (s, 1H, CH-pyrimidine), 7.1–7.7 (m, 8H, aromatic), 8.1, 9.6 (2 s, 2H, 2NH (D_2O exchangeable)), 10.2 (s, 1H, CONH (D_2O exchangeable)). ^{13}C NMR: (DMSO-d_6, 400 MHz) δ (ppm): 175.32, 164.56, 157.56, 144.45, 138.22, 131.44, 130.96, 128.34, 127.64, 127.34, 121.63, 115.63, 111.93, 106.42, 54.34, 21.54, 17.45; MS (EI) *m/z*: 362.04 (M^+, 22.1%). Anal. Calcd., for $C_{20}H_{18}N_4OS$: C, 66.28; H, 5.01; N, 15.46. Found: C, 66.34; H, 5.04; N, 15.52.

4-(2-cyanophenyl)-6-methyl-*N*-(4–fluorophenyl)-2-thioxo-1,2,3,4-tetrahydropyrimidine-5-carboxamide 7c:

Yield: 75%; m.p.: 270–272 °C; IR ν (KBr cm^{-1}): 3377, 3270 (NH), 3164 (CH, aromatic), 2980 (CH, aliphatic), 1675 (C═O), 1270 (C═S). ^{1}HNMR (DMSO-d_6, 400 MHz) δ: 2.3 (s, 3H, CH_3), 5.2 (s, 1H, CH-pyrimidine), 7.2–7.8, (m, 8H, aromatic), 7.9, 9.5 (2 s, 2H, 2NH (D_2O exchangeable)), 9.9 (s, 1H, CONH (D_2O exchangeable)). ^{13}C NMR: (DMSO-d_6, 400 MHz) δ (ppm): 175.24, 163.13, 162.91, 159.14, 149.54, 133.43, 133.21, 132.41, 127.63, 127.42, 126.16, 115.85, 115.87, 111.54, 106.53, 54.96, 17.9; MS (EI) *m/z*: 366.18 (M^+, 27.3%). Anal. Calcd., for $C_{19}H_{15}FN_4OS$: C, 62.28; H, 4.13; N, 15.29. Found: C, 62.39; H, 4.24; N, 15.32.

4-(2-chlorophenyl)-6-methyl-*N*-phenyl-2-thioxo-1,2,3,4-tetrahydropyrimidine-5-carboxamide 8a:

Yield: 69%; m.p.: 256–258 °C.

4-(2-chlorophenyl)-6-methyl-*N*-(4-methylphenyl)-2-thioxo-1,2,3,4-tetrahydropyrimidine-5-carboxamide 8b:

Yield: 60%; m.p.: 245–247 °C; IR ν (KBr cm^{-1}): 3383, 3272 (NH), 3190 (CH, aromatic), 2979 (CH, aliphatic), 1675 (C═O), 1270 (C═S). ^{1}HNMR (DMSO-d_6, 400 MHz) δ: 2.3 (s, 3H, CH_3), 2.8 (s, 3H, CH_3), 5.6 (s, 1H, CH pyrimidine), 7.1–7.8 (m, 8H, aromatic), 7.9, 9.1 (2 s, 2H, 2NH (D_2O exchangeable)), 9.8 (s, 1H, CONH (D_2O exchangeable)). ^{13}C NMR: (DMSO-d_6, 400 MHz) δ (ppm): 175.45, 163.22, 158.45, 142.78, 136.76, 134.87, 132.65, 128.72, 128.65, 128.05, 126.76, 121.54, 104.56, 54.34, 22.76, 19.45; Anal. Calcd., for $C_{19}H_{18}ClN_3OS$: C, 61.37; H, 4.88; N, 11.30. Found: C, 61.29; H, 4.74; N, 11.36.

4-(2-chlorophenyl)-6-methyl-*N*-(4-fluoro phenyl-2-thioxo-1,2,3,4-tetrahydro pyrimidine-5-carboxamide 8c:

Yield: 67%; m.p.: 257–259 °C.

4-(2-bromophenyl)-6-methyl-*N*-phenyl-2-thioxo-1,2,3,4-tetrahydropyrimidine-5-carboxamide 9a:

Yield: 73%; m.p.: 248–250 °C.

4-(2-bromophenyl)-*N*-(4–methyphenyl)-6-methyl-2-thioxo-1,2,3,4-tetrahydro pyrimidine-5-carboxamide 9b:

Yield: 67%; m.p.: 262–264 °C.

4-(2-bromophenyl)-6-methyl-*N*-(4-fluorophenyl-2-thioxo-1,2,3,4-tetrahydropyrimidine-5-carboxamide 9c:

Yield: 76%; m.p.: 281–283 °C.

4.2. Biological evaluation

4.2.1. Evaluation of the antihypertensive activity

4.2.1.1. Animals. Male Wistar albino rats (200–250 g), were purchased from VACSERA (Helwan, Cairo, Egypt).

Animals were housed in plastic cages with free access to food and water under standard conditions of temperature and humidity with an alternating 12 h light and dark cycle. The study protocol was approved by the Animal Ethics Committee of the Faculty of Pharmacy, Helwan University and was conducted according to the guidelines of the EC, directive 86/609/EEC for animal experiments.

4.2.1.2. Direct arterial pressure measurement. Rats were fasted overnight and anesthetized by i.p. injection of Pentothal sodium (80 mg/Kg). For each animal, the reflexes were checked, and the rat was placed on a proper rodent surgical table. The ventral side of the neck, right hind leg, and chest were cautiously disinfected then shaved. A small incision (1.5–2 cm) was made in the neck of the rats for carotid artery cannulation. The carotid artery was cannulated using a cannula pre-filled with heparinized normal saline (0.5 IU/mL) and attached to blood pressure transducer to record the arterial blood pressure. Three hours prior to cannulation, animals were treated with the test drugs, nifedipine or normal saline in the control group at a dose of 0.3 mL. Following cannulation, the sensor was connected to the Power Lab instrument and the blood pressure was recorded and analyzed [65].

4.2.2. Calcium antagonism in the isolated rat ileum

4.2.2.1. Ileum segment preparation and recording of the contraction.. Tissue segments' isolation and ileal spasmolytic activity estimation were achieved as previously described [66]. After overnight fasting, rats were sacrificed by cervical dislocation and the terminal ileum was dissected out and stored in Tyrode's solution (136.89 mM NaCl, 2.68 mM KCl, 1.05 mM MgCl2, 1.80 mM CaCl2, 0.42 mM NaH2PO4, 11.09 mM NaHCO3 and 5.55 mM glucose; pH 7.4). The mesentery of ileum was removed. Each 2-cm-long segment was suspended in a 25-mL tissue bath containing Tyrode's solution at 37 °C and constantly aerated with 5% (v/v) CO_2 in oxygen. One end of the isolated ileum was attached to the bath bottom, while the other one to an isotonic force transducer (TSZ-04-E, Experimetria Ltd., Budapest, Hungary). Intestinal responses were recorded and analyzed with a SPEL Advanced ISOSYS Data Acquisition System (Experimetria Ltd.). Tissues were allowed to stabilize for 30 min before the experiment. After each assay, the tissue was washed with fresh Tyrode's solution and equilibrated for about 10 min.

To assess the possible Ca^{2+} channel blocking effects of the test compounds, a solution containing K^+ (80 mM) was added to the bath with rat ileum to produce a sustained contraction. The test compounds (0.1–0.5 mL) were cumulatively added to the tissue bath. The relaxation of K^+ induced ileum contraction was expressed as the percentage change in the control response caused by K^+ for each concentration of the test

compounds and standard (Nifedipine). IC_{50} dose was calculated by dose response inhibitory curve using GraphPad Prism version 5 for Windows (GraphPad Inc., USA) and the conc of the test compound causing 50% inhibition was calculated according to the following equation:

IC_{50} (μg/mL) = dose for 50% inhibition (mL) × conc. (1000 μg/mL) ÷ bath capacity (25 mL)

4.2.3. *In vitro ACE2: spike RBD (SARS-CoV-2) inhibitor screening Colorimetric assay*

In order to measure Angiotensin-Converting Enzyme 2 (ACE2) receptor inhibition activity, the ACE2:SARS-CoV-2 Spike (RBD) Inhibitor Screening Colorimetric Assay Kit # 78031 (Bps Bioscience, Cornerstone Court W, Ste B San Diego, CA 92121) was used. This Kit is designed for screening and profiling inhibitors of the interaction between the Spike protein of SARS-CoV-2 and ACE2 receptor [13,67]. The assay was performed according to manufacturer's instruction. First, ACE2 protein was attached to a clear nickel-coated 96-well plate. Next, SARS-CoV-2 Spike-Fc was incubated with ACE2 with or without the test inhibitor (5–50 nM) on the plate. Finally, the plate was treated with HRP-labeled anti-Fc, followed by addition of an HRP substrate to produce color, which was then measured at 450 nm using a UV/Vis spectrophotometer microplate reader. All experiments were performed in triplicates. IC_{50} was calculated by dose response inhibitory curve using GraphPad Prism version 5 for Windows (GraphPad Inc., USA).

4.2.4. *In vitro anti-inflammatory evaluation*

4.2.4.1. Cell culture and differentiation. The THP-1 cell line was obtained from Nawah Scientific (Cairo, Egypt) and maintained at a concentration of 1×10^5 cells/mL in RPMI 1640 containing 10% fetal calf serum (FCS), 2 mmol/L L-glutamine and 100 IU/100 μg/mL penicillin/streptomycin. The cells were sub-cultured every 2 days using fresh media and maintained in an incubator at 37 °C, 5% CO_2 and 100% humidity. THP-1 cells were differentiated using Phorbol 12-myristate 13-acetate (PMA), (Sigma-Aldrich, St. Louis, USA) at concentration of 60 ng/mL and incubated for 48 h. THP-1 cell differentiation was developed by replacing the PMA-containing media with fresh media for a further 24 h. Cells were examined under a light microscope for the evidence of differentiation.

4.2.4.2. PMA-differentiated THP-1 cell viability assay. Differentiated THP-1 cells were seeded in 96-well plates at a density of 1×10^5 cells/well and incubated at 37 °C for 24 h in a humidified atmosphere containing 5% CO_2. After 24 h, the cells were treated with different concentrations (1–2000 μg/mL) of test compounds (**5a, 5b, 6a, 6b, 7a, 7b, 8a, 8c** and **9a**). Untreated cells and medium were used as control and blank, respectively. After incubation for 24 h, the number of viable cells were determined by the MTT test. Briefly, the culture medium was removed and replaced with 100 μl of fresh culture RPMI 1640 medium without phenol red then 10 μl of the 12 mM MTT stock solution (5 mg of MTT in 1 mL of PBS) was added to each well. The plates were then incubated at 37 °C and 5% CO_2 for 4 h. An 85 μl aliquot of the media was removed from the wells, and 50 μl of DMSO was added to each well and mixed thoroughly with the pipette then incubated at 37 °C for 10 min. The optical density was measured at 590 nm with the microplate reader (SunRise, TECAN, Inc, USA). GraphPad Prism for Windows (version 5.00, GraphPad Inc, CA, USA) was used to obtain dose–response curves and mean inhibitory concentration (IC_{50}) values.

4.2.4.3. Detection of pro-inflammatory cytokine IL-6 and CRP production. After 48 h of THP-1 cells differentiation using PMA (60 ng/mL) in 24-well plates, the media were aspirated, and the cells were incubated in PMA-free medium for additional 24 h. At the 4th day, THP-1 cells were incubated in the presence or absence of compounds **5a, 7a,b,** and **9a** below their IC_{50}, which were added 2 h prior to treatment with LPS at 0.5 μg/mL (Sigma-Aldrich, St. Louis, USA) for further 24 h. Finally, conditioned media were collected and frozen pending ELISA (n = 3).

4.2.4.4. Enzyme-linked immunosorbent assay (ELISA). To quantify the release of inflammatory cytokine IL-6 in cell culture supernatants, ELISA Ready-Set-Go kits were purchased from Thermo Fisher Scientific (Loughborough, UK). While human C-reactive protein (CRP) was determined using High Sensitivity Human CRP ELISA Kit (Anogen, ON, Canada). The assays were performed according to the manufacturer's instructions. The plates were read at 560 and 450 nm, respectively.

4.2.5. *Statistical analysis*

Mean and SD values were calculated for each group, and the comparison between the groups was performed by one way ANOVA followed by *post-hoc* test, using GraphPad InStat software version 3.05 (GraphPad Inc., La Jolla, CA, USA). A probability value of $P < 0.05$ was considered significant.

Declaration of Competing Interest

The authors declare that they have no known competing financial interests or personal relationships that could have appeared to influence the work reported in this paper.

Acknowledgement

Herein, we extend our profound appreciation to our colleagues in department of Pharmacology and Toxicology, Faculty of Pharmacy, Helwan University for their help during the experimental part involving the animals.

Appendix A. Supplementary material

Supplementary data to this article can be found online at https://doi.org/10.1016/j.bioorg.2021.105272.

References

[1] M. Tadic, S. Saeed, G. Grassi, S. Taddei, G. Mancia, C. Cuspidi, Hypertension and COVID-19: ongoing controversies, Front. Cardiovasc. Med. 8 (2021), 639222, https://doi.org/10.3389/fcvm.2021.639222.
[2] A.D. Sinha, R. Agarwal, Clinical pharmacology of antihypertensive therapy for the treatment of hypertension in CKD, Clin. J. Am. Soc. Nephrol. 14 (5) (2019) 757–764, https://doi.org/10.2215/CJN.04330418.
[3] G. Gheorghe, M. Ilie, S. Bungau, A.M.P. Stoian, N. Bacalbasa, C.C. Diaconu, Is There a Relationship between COVID-19 and Hyponatremia? Medicina (Kaunas) 57 (1) (2021) 55, https://doi.org/10.3390/medicina57010055.
[4] T. Godfraind, Discovery and development of calcium channel blockers, Front Pharmacol. 8 (2017) 286, https://doi.org/10.3389/fphar.2017.00286.
[5] J.D. Parker, M. D' Iorio, J.S. Floras, C.B. Toal, Comparison of short-acting versus extended-release nifedipine: effects on hemodynamics and sympathetic activity in patients with stable coronary artery disease, Sci. Rep. 10 (1) (2020), https://doi.org/10.1038/s41598-019-56890-1.
[6] Y. Kawabata, T. Soeki, H. Ito, T. Matsuura, K. Kusunose, T. Ise, K. Yamaguchi, T. Tobiume, S. Yagi, D. Fukuda, H. Yamada, T. Wakatsuki, M. Kitani, K. Kawano, Y. Taketani, M. Sata, F. Morello, Effects of L-/N-type calcium channel blockers on angiotensin II–renin feedback in hypertensive patients, Int. J. Hypertension 2020 (2020) 1–7.
[7] D. Pugh, P.J. Gallacher, N. Dhaun, Management of hypertension in chronic kidney disease, Drugs 79 (4) (2019) 365–379, https://doi.org/10.1007/s40265-019-1064-1.
[8] N.E. Clarke, A.J. Turner, Angiotensin-converting enzyme 2: the first decade, Int. J. Hypertens 2012 (2012) 1–12, https://doi.org/10.1155/2012/307315.
[9] V.B. Patel, J.-C. Zhong, M.B. Grant, G.Y. Oudit, Role of the ACE2/angiotensin 1–7 axis of the renin–angiotensin system in heart failure, Circ. Res. 118 (8) (2016) 1313–1326, https://doi.org/10.1161/CIRCRESAHA.116.307708.
[10] P.K. Datta, F. Liu, T. Fischer, J. Rappaport, X. Qin, SARS-CoV-2 pandemic and research gaps: Understanding SARS-CoV-2 interaction with the ACE2 receptor and implications for therapy, Theranostics 10 (16) (2020) 7448–7464, https://doi.org/10.7150/thno.48076.
[11] R.A.S. Santos, A.J. Ferreira, A.C. Simões e Silva, Recent advances in the angiotensin-converting enzyme 2–angiotensin (1–7)–Mas axis, Experimental physiology 93(5) (2008) 519-527. https://doi.org/10.1113/expphysiol.2008.042002.

[12] Z. Abassi, Y. Knaney, T. Karram, S.N. Heyman, The lung macrophage in SARS-CoV-2 infection: a friend or a foe? Front Immunol 11 (2020) 1312, https://doi.org/10.3389/fimmu.2020.01312.
[13] M. Hoffmann, H. Kleine-Weber, S. Schroeder, N. Krüger, T. Herrler, S. Erichsen, T. S. Schiergens, G. Herrler, N.-H. Wu, A. Nitsche, M.A. Müller, C. Drosten, S. Pöhlmann, SARS-CoV-2 cell entry depends on ACE2 and TMPRSS2 and is blocked by a clinically proven protease inhibitor, Cell 181 (2) (2020) 271–280.e8, https://doi.org/10.1016/j.cell.2020.02.052.
[14] W. Li, M.J. Moore, N. Vasilieva, J. Sui, S.K. Wong, M.A. Berne, M. Somasundaran, J.L. Sullivan, K. Luzuriaga, T.C. Greenough, H. Choe, M. Farzan, Angiotensin-converting enzyme 2 is a functional receptor for the SARS coronavirus, Nature 426 (6965) (2003) 450–454, https://doi.org/10.1038/nature02145.
[15] M. Hoffmann, H. Kleine-Weber, N. Krüger, M.A. Mueller, C. Drosten, S. Pöhlmann, The novel coronavirus 2019 (2019-nCoV) uses the SARS-coronavirus receptor ACE2 and the cellular protease TMPRSS2 for entry into target cells, BioRxiv (2020), https://doi.org/10.1101/2020.01.31.929042.
[16] A.C. Walls, Y.-J. Park, M.A. Tortorici, A. Wall, A.T. McGuire, D. Veesler, Structure, function, and antigenicity of the SARS-CoV-2 spike glycoprotein, Cell 181 (2) (2020) 281–292, https://doi.org/10.1016/j.cell.2020.02.058.
[17] Y. Ji, Z. Wang, Z. Li, A. Zhang, Y. Jin, H. Chen, et al., Angiotensin II enhances proliferation and inflammation through AT1/PKC/NF-kappaB signaling pathway in hepatocellular carcinoma cells, Cell Physiol. Biochem. 39 (1) (2016) 13–32, https://doi.org/10.1159/000445602.
[18] H. Okamoto, N. Ichikawa, The pivotal role of the angiotensin-II-NF-kappaB axis in the development of COVID-19 pathophysiology, Hypertens Res/ 44 (1) (2021) 126–128, https://doi.org/10.1038/s41440-020-00560-7.
[19] T. Hirano, M. Murakami, COVID-19: a new virus, but a familiar receptor and cytokine release syndrome, Immunity 52 (5) (2020) 731–733, https://doi.org/10.1016/j.immuni.2020.04.003.
[20] T. Behl, I. Kaur, S. Bungau, A. Kumar, M.S. Uddin, C. Kumar, G. Pal, Sahil, K. Shrivastava, G. Zengin, S. Arora, The dual impact of ACE2 in COVID-19 and ironical actions in geriatrics and pediatrics with possible therapeutic solutions, Life Sci 257 (2020) 118075, https://doi.org/10.1016/j.lfs.2020.118075.
[21] C.M. Bhalgat, M.I. Ali, B. Ramesh, G. Ramu, Novel pyrimidine and its triazole fused derivatives: synthesis and investigation of antioxidant and anti-inflammatory activity, Arabian J. Chem. 7 (6) (2014) 986–993, https://doi.org/10.1016/j.arabjc.2010.12.021.
[22] R. Kaur, S. Chaudhary, K. Kumar, M.K. Gupta, R.K. Rawal, Recent synthetic and medicinal perspectives of dihydropyrimidinones: a review, Eur. J. Med. Chem. 132 (2017) 108–134, https://doi.org/10.1016/j.ejmech.2017.03.025.
[23] A.M. Farghaly, O.M. AboulWafa, Y.A.M. Elshaier, W.A. Badawi, H.H. Haridy, H.A. E. Mubarak, Design, synthesis, and antihypertensive activity of new pyrimidine derivatives endowing new pharmacophores, Med. Chem. Res. 28 (3) (2019) 360–379, https://doi.org/10.1007/s00044-019-02289-6.
[24] N. Irshad, A.-U. Khan, Alamgeer, S.-U.-D. Khan, M.S. Iqbal, Antihypertensive potential of selected pyrimidine derivatives: explanation of underlying mechanistic pathways, Biomed. Pharmacother. 139 (2021) 111567, https://doi.org/10.1016/j.biopha.2021.111567.
[25] M.A. Abu-Zaied, G.H. Elgemeie, N.M. Mahmoud, Anti-covid-19 drug analogues: synthesis of novel pyrimidine thioglycosides as antiviral agents against SARS-COV-2 and avian influenza H5N1 viruses, ACS Omega 6 (26) (2021) 16890–16904, https://doi.org/10.1021/acsomega.1c0150110.1021/acsomega.1c01501.s001.
[26] M.A. Abu-Zaied, N.M. Mahmoud, G.H. Elgemeie, Toward developing therapies against corona virus: synthesis and anti-avian influenza virus activity of novel cytosine thioglycoside analogues, ACS Omega 5 (32) (2020) 20042–20050, https://doi.org/10.1021/acsomega.0c0153710.1021/acsomega.0c01537.s001.
[27] C.O. Kappe, A. Stadler, The B iginelli Dihydropyrimidine Synthesis, Org. React. 63 (2004) 1–116, https://doi.org/10.1002/0471264180.or063.01.
[28] H. Nagarajaiah, A. Mukhopadhyay, J.N. Moorthy, Biginelli reaction: an overview, Tetrahedron Lett. 57 (47) (2016) 5135–5149, https://doi.org/10.1016/j.tetlet.2016.09.047.
[29] J. Bais, F. Benedetti, F. Berti, I. Cerminara, S. Drioli, M. Funicello, G. Regini, M. Vidali, F. Felluga, One pot synthesis of micromolar BACE-1 inhibitors based on the dihydropyrimidinone scaffold and their thia and imino analogues, Molecules 25 (18) (2020) 4152, https://doi.org/10.3390/molecules25184152.
[30] M. Damgaard, A. Al-Khawaja, M. Nittegaard-Nielsen, R.F. Petersen, P. Wellendorph, B. Frølund, Monastrol, a 3, 4-dihydropyrimidin-2 (1H)-thione, as structural scaffold for the development of modulators for GHB high-affinity binding sites and α1β2δ GABAA receptors, Eur. J. Med. Chem. 138 (2017) 300–312, https://doi.org/10.1016/j.ejmech.2017.06.024.
[31] T.C. Braga, I.C.G. de Jesus, K.V. Soares, S. Guatimosim, L. da Silva Neto, C.J. da-Silva, et al., A novel H 2 S releasing-monastrol hybrid (MADTOH) inhibits L-type calcium channels, New Journal of Chemistry 45(2) (2021) 671-678. https://doi.org/10.1039/D0NJ04415F.
[32] H.A. Katouah, H.E. Gaffer, Synthesis and docking study of pyrimidine derivatives scaffold for anti-hypertension application, ChemistrySelect 4 (20) (2019) 6250–6255, https://doi.org/10.1002/slct.v4.2010.1002/slct.201900799.
[33] K.S. Jain, J.B. Bariwal, M.K. Kathiravan, M.S. Phoujdar, R.S. Sahne, B.S. Chauhan, A.K. Shah, M.R. Yadav, Recent advances in selective α1-adrenoreceptor antagonists as antihypertensive agents, Bioorg. Med. Chem. 16 (9) (2008) 4759–4800, https://doi.org/10.1016/j.bmc.2008.02.091.
[34] A.C. Dolphin, Functions of presynaptic voltage-gated calcium channels, Function (Oxf) 2 (1) (2021) zqaa027, https://doi.org/10.1093/function/zqaa027.
[35] N. Negrut, A. Codrean, I. Hodisan, S. Bungau, D. Tit, R. Marin, T. Behl, F. Banica, C. Diaconu, D. Nistor-Cseppento, Efficiency of antiviral treatment in COVID-19, Exp Ther Med 21 (6) (2021), https://doi.org/10.3892/etm10.3892/etm.2021.10080.
[36] R. Dalan, S.R. Bornstein, A. El-Armouche, R.N. Rodionov, A. Markov, B. Wielockx, F. Beuschlein, B.O. Boehm, The ACE-2 in COVID-19: foe or friend? Horm. Metab. Res. 52 (05) (2020) 257–263, https://doi.org/10.1055/a-1155-0501.
[37] Z. Abassi, S.K. Abd Al Roof Higazi, Z. Armaly, K. Skorecki, S.N. Heyman, ACE2, COVID-19 Infection, Inflammation, and Coagulopathy: Missing Pieces in the Puzzle, Frontiers in physiology 11 (2020). https://doi.org/10.3389/fphys.2020.574753.
[38] M. Daigneault, J.A. Preston, H.M. Marriott, M.K.B. Whyte, D.H. Dockrell, T. M. Doherty, The identification of markers of macrophage differentiation in PMA-stimulated THP-1 cells and monocyte-derived macrophages, PLoS ONE 5 (1) (2010) e8668, https://doi.org/10.1371/journal.pone.0008668.
[39] E.K. Park, H.S. Jung, H.I. Yang, M.C. Yoo, C. Kim, K.S. Kim, Optimized THP-1 differentiation is required for the detection of responses to weak stimuli, Inflamm. Res. 56 (1) (2007) 45–50, https://doi.org/10.1007/s00011-007-6115-5.
[40] H. Gilzad-Kohan, F. Jamali, Anti-inflammatory properties of drugs used to control covid-19 and their effects on the renin-angiotensin system and angiotensin-converting Enzyme-2, J. Pharm. Pharm. Sci. 23 (2020) 259–277, https://doi.org/10.18433/jpps31346.
[41] A. Jafarzadeh, P. Chauhan, B. Saha, S. Jafarzadeh, M. Nemati, Contribution of monocytes and macrophages to the local tissue inflammation and cytokine storm in COVID-19: Lessons from SARS and MERS, and potential therapeutic interventions, Life Sci. 257 (2020) 118102, https://doi.org/10.1016/j.lfs.2020.118102.
[42] D.M. Del Valle, S. Kim-Schulze, H.-H. Huang, N.D. Beckmann, S. Nirenberg, B. o. Wang, Y. Lavin, T.H. Swartz, D. Madduri, A. Stock, T.U. Marron, H. Xie, M. Patel, K. Tuballes, O. Van Oekelen, A. Rahman, P. Kovatch, J.A. Aberg, E. Schadt, S. Jagannath, M. Mazumdar, A.W. Charney, A. Firpo-Betancourt, D.R. Mendu, J. Jhang, D. Reich, K. Sigel, C. Cordon-Cardo, M. Feldmann, S. Parekh, M. Merad, S. Gnjatic, An inflammatory cytokine signature predicts COVID-19 severity and survival, Nat. Med. 26 (10) (2020) 1636–1643, https://doi.org/10.1038/s41591-020-1051-9.
[43] M.T. Kabir, M.S. Uddin, M.F. Hossain, J.A. Abdulhakim, M.A. Alam, G.M. Ashraf, S. G. Bungau, M.N. Bin-Jumah, M.M. Abdel-Daim, L. Aleya, nCOVID-19 pandemic: from molecular pathogenesis to potential investigational therapeutics, Front Cell Dev. Biol. 8 (2020), https://doi.org/10.3389/fcell.2020.00616.
[44] N.R. Sproston, J.J. Ashworth, Role of C-Reactive Protein at Sites of Inflammation and Infection, Front Immunol 9 (2018) 754, https://doi.org/10.3389/fimmu.2018.00754.
[45] A.K. Shrivastava, H.V. Singh, A. Raizada, S.K. Singh, C-reactive protein, inflammation and coronary heart disease, Egypt. Heart J. 67 (2) (2015) 89–97, https://doi.org/10.1016/j.ehj.2014.11.005.
[46] A. Warusevitane, D. Karunatilake, J. Sim, C. Smith, C. Roffe, E. Gándara, Early diagnosis of pneumonia in severe stroke: clinical features and the diagnostic role of C-reactive protein, PLoS ONE 11 (3) (2016) e0150269, https://doi.org/10.1371/journal.pone.0150269.
[47] D. Vasileva, A. Badawi, C-reactive protein as a biomarker of severe H1N1 influenza, Inflamm. Res. 68 (1) (2019) 39–46, https://doi.org/10.1007/s00011-018-1188-x.
[48] L. Badimon, E. Pena, G. Arderiu, T. Padro, M. Slevin, G. Vilahur, et al., C-reactive protein in atherothrombosis and angiogenesis, Front Immunol 9 (2018) 430, https://doi.org/10.3389/fimmu.2018.00430.
[49] X. Luo, W. Zhou, X. Yan, T. Guo, B. Wang, H. Xia, et al., Prognostic value of C-reactive protein in patients with coronavirus 2019, Clinical Infectious Diseases 71 (16) (2020) 2174-2179. https://doi.org/10.1093/cid/ciaa641.
[50] F. Liu, L. Li, M. Xu, J. Wu, D. Luo, Y. Zhu, et al., Prognostic value of interleukin-6, C-reactive protein, and procalcitonin in patients with COVID-19, J. Clin. Virol. 127 (2020), 104370, https://doi.org/10.1016/j.jcv.2020.104370.
[51] C. Wu, X. Chen, Y. Cai, X. Zhou, S. Xu, H. Huang, et al., Risk factors associated with acute respiratory distress syndrome and death in patients with coronavirus disease 2019 pneumonia in Wuhan, China, JAMA Int. Med. 180 (7) (2020) 934–943, https://doi.org/10.1001/jamainternmed.2020.0994.
[52] J. Geleris, Y. Sun, J. Platt, J. Zucker, M. Baldwin, G. Hripcsak, et al., Observational study of hydroxychloroquine in hospitalized patients with Covid-19, The New England J. Med. 382 (25) (2020) 2411–2418, https://doi.org/10.1056/NEJMoa2012410.
[53] J. Fantini, C. Di Scala, H. Chahinian, N. Yahi, Structural and molecular modelling studies reveal a new mechanism of action of chloroquine and hydroxychloroquine against SARS-CoV-2 infection, Int. J. Antimicrob. Agents 55 (5) (2020), 105960, https://doi.org/10.1016/j.ijantimicag.2020.105960.
[54] I. Solaimanzadeh, Nifedipine and amlodipine are associated with improved mortality and decreased risk for intubation and mechanical ventilation in elderly patients hospitalized for COVID-19, Cureus 12 (5) (2020), e8069, https://doi.org/10.7759/cureus.8069.
[55] M.A. Zolfigol, H. Ghaderi, S. Baghery, L. Mohammadi, Nanometasilica disulfuric acid (NMSDSA) and nanometasilica monosulfuric acid sodium salt (NMSMSA) as two novel nanostructured catalysts: applications in the synthesis of Biginelli-type, polyhydroquinoline and 2, 3-dihydroquinazolin-4 (1 H)-one derivatives, J. Iran. Chem. Soc. 14 (1) (2017) 121–134, https://doi.org/10.1007/s13738-016-0964-1.
[56] S.A. Abdel-Aziz, N.A. El-Koussi, H.Y. Hassan, A.F. Youssef, M.M. Yousri, Synthesis of substituted dihydropyrimidines as hypotensive agents, Bull. Pharm. Sci. Assiut 34 (2) (2011) 159–179, https://doi.org/10.21608/bfsa.2011.63272.
[57] B. Ahmed, R.A. Khan, M. Keshari, An improved synthesis of Biginelli-type compounds via phase-transfer catalysis, Tetrahedron Lett. 50 (24) (2009) 2889–2892, https://doi.org/10.1016/j.tetlet.2009.03.177.

[58] P. Kakati, P. Singh, P. Yadav, S.K. Awasthi, Aiding the versatility of simple ammonium ionic liquids by the synthesis of bioactive 1, 2, 3, 4-tetrahydropyrimidine, 2-aminothiazole and quinazolinone derivatives, New J. Chem. 45 (15) (2021) 6724–6738, https://doi.org/10.1039/D1NJ00280E.
[59] K. Malani, S.S. Thakkar, M.C. Thakur, A. Ray, H. Doshi, Synthesis, characterization and in silico designing of diethyl-3-methyl-5-(6-methyl-2-thioxo-4-phenyl-1, 2, 3, 4-tetrahydropyrimidine-5-carboxamido) thiophene-2, 4-dicarboxylate derivative as anti-proliferative and anti-microbial agents, Bioorg. Chem. 68 (2016) 265–274, https://doi.org/10.1016/j.bioorg.2016.09.001.
[60] V.L. Gein, I.V. Kholkin, T.M. Zamaraeva, E.V. Voronina, M.I. Vakhrin, Synthesis and antimicrobial activity of N, 6-diaryl-4-methyl-2-thioxo-1, 2, 3, 6-tetrahydropyrimidine-5-carboxamides, Pharm. Chem. J. 46 (2) (2012) 114–116, https://doi.org/10.1007/s11094-012-0743-y.
[61] V.R. Virsodia, N.R. Vekariya, A.T. Manvar, R.C. Khunt, B.R. Marvania, B.S. Savalia, et al., Catalyst-free, rapid synthesis of fused bicyclic thiazolo-pyrimidine and pyrimido-thiazine derivatives by a microwave-assisted method, Phosphorus, Sulfur, and Silicon and the Related Elements 184 (1) (2008) 34–44, https://doi.org/10.1080/10426500802077564.
[62] https://pubchem.ncbi.nlm.nih.gov/compound/1038182.
[63] https://pubchem.ncbi.nlm.nih.gov/compound/1111622.
[64] https://pubchem.ncbi.nlm.nih.gov/compound/1291746.
[65] S. Parasuraman, R. Raveendran, Measurement of invasive blood pressure in rats, J. Pharmacol. Pharmacotherapeut. 3 (2) (2012) 172, https://doi.org/10.4103/0976-500X.95521.
[66] D.R. Pavlović, S. Branković, N. Kovačević, D. Kitić, S. Veljković, Comparative study of spasmolytic properties, antioxidant activity and phenolic content of Arbutus unedo from Montenegro and Greece, Phytother. Res. 25 (5) (2011) 749–754, https://doi.org/10.1002/ptr.3460.
[67] R. Yan, Y. Zhang, Y. Li, L. Xia, Y. Guo, Q. Zhou, Structural basis for the recognition of SARS-CoV-2 by full-length human ACE2, Science 367 (6485) (2020) 1444–1448, https://doi.org/10.1126/science.abb2762.